

A Solid-State 0.56 THz Near-Field Array for μM -Scale Surface Imaging

Philipp Hillger¹, Ritesh Jain¹, Janusz Grzyb¹, Laven Mavarani¹, Thomas Bücher¹, Gaetan Mac Grogan², Patrick Mounaix³, Jean-Paul Guillet³, Ullrich R. Pfeiffer¹

¹IHCT, University of Wuppertal, Germany, ²Institut Bergonié, Bordeaux, France, ³IMS CNRS 5218, Talence, France

Abstract—We demonstrate a fully-integrated 0.56 THz 128-pixel near-field 1-D sensor array with 10-12 μm lateral resolution. The sensing elements are based two parallel cross-bridged split-ring resonators that utilize a 3-D topology to exhibit high field confinement in the sensing spot. The sensor comprises a scalable excitation scheme that is designed to maximize the fill factor of the imager for large 1-D arrays. The THz front-end is co-integrated with a digital-read out chain. This enables rapid THz near-field image acquisition of planar and soft surfaces. Furthermore, the imager can be operated as a standalone device that is only powered with a USB cable. As an exemplary application, this work demonstrates THz near-field sensing as a tool for biometric fingerprint reading for the first time.

I. INTRODUCTION

TODAY'S super-resolution THz imaging systems are based on near-field scanning microscopy (NSOM). NSOM techniques are most commonly based on sampling of the near-field interaction of a narrow aperture [1] or scattering probe-tip [2] with a sample. Lateral resolutions in the nm-range have been demonstrated, with the record values of 20-40 nm achieved with AFM-tips [2]. This makes NSOM an essential technique for fundamental THz research. However, NSOM suffers from low dynamic range and long integration times due to the poor optical coupling efficiency between THz illumination, detection and the sensing spot. This leads to challenging radiation power and sensitivity requirements on the source and detector side, respectively, as well as bulky and expensive components.

Recently presented silicon-based THz near-field sensors address these shortcomings by combining illumination, detection and near-field sensing on a single silicon die [3][4]. They are based on object-dependent power transmission modulation of an on-chip generated THz wave through a 3-D split-ring resonator (SRR). The sensors offer high sensitivity, low-cost and standalone operation, which are ultimately necessary to leverage usage of THz near-field sensors in practical imaging applications. However, these are only single pixel implementations, and hence they require large image acquisition times. Furthermore, the presented sensors comprise only the THz front-end and thus do not fully exploit the mixed signal integration capabilities of modern nanoscale silicon technology. This work shows a fully integrated system-on-a-chip for THz near-field sensing and scales up the research of THz near-field sensing into larger surfaces with numerous pixels [5].

II. SENSOR DESIGN

The chip is implemented in a high-speed 0.13 μm SiGe BiCMOS technology that allows co-integration of a large-scale THz front-end and analog/digital post-processing on the same die [6]. Fig. 1 shows the micrograph of the chip and Fig.

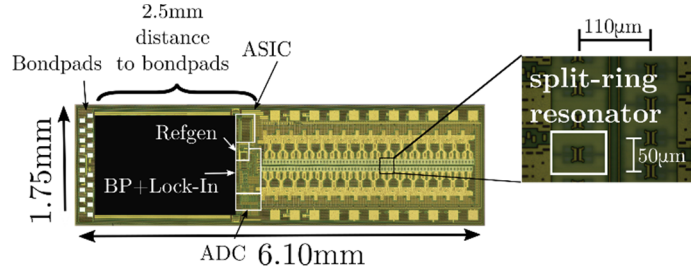


Fig. 1. Micrograph of the near-field array. The length of the sensing area is 3.2 mm.

2 shows the top-level block diagram of the sensor. Core of each pixel is the previously presented cross-bridged double SRR with 10-12 μm lateral resolution shown in Fig. 3a) [4] that is incoherently excited close to resonance by a free running on-chip oscillator source. The SRR exposes a highly-confined electric-dipole type field to the top surface of the chip. As illustrated in Fig. 3c), object placement in the sensing volume causes a dielectric-permittivity based modulation of the transmitted power, which is detected with a SiGe-HBT THz power detector exploiting the nonlinearity of the base-emitter junction for rectification. The pixels are grouped into 32 subarrays of 4 pixels that each share a 534-562 GHz triple-push oscillator (TPO) for excitation through two cascaded

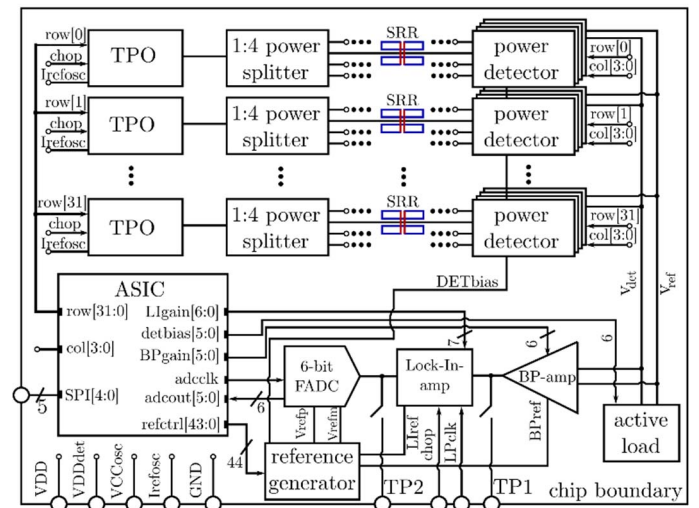


Fig. 2. Top-level block diagram of the near-field array. The chip includes all functions such as illumination, sensing, detection, and digital readout on a single silicon chip.

modified Wilkinson power dividers. Only the field in the gap of the SRRs is exposed to the chip top surface, while all other electromagnetic fields are shielded from the sensing plane

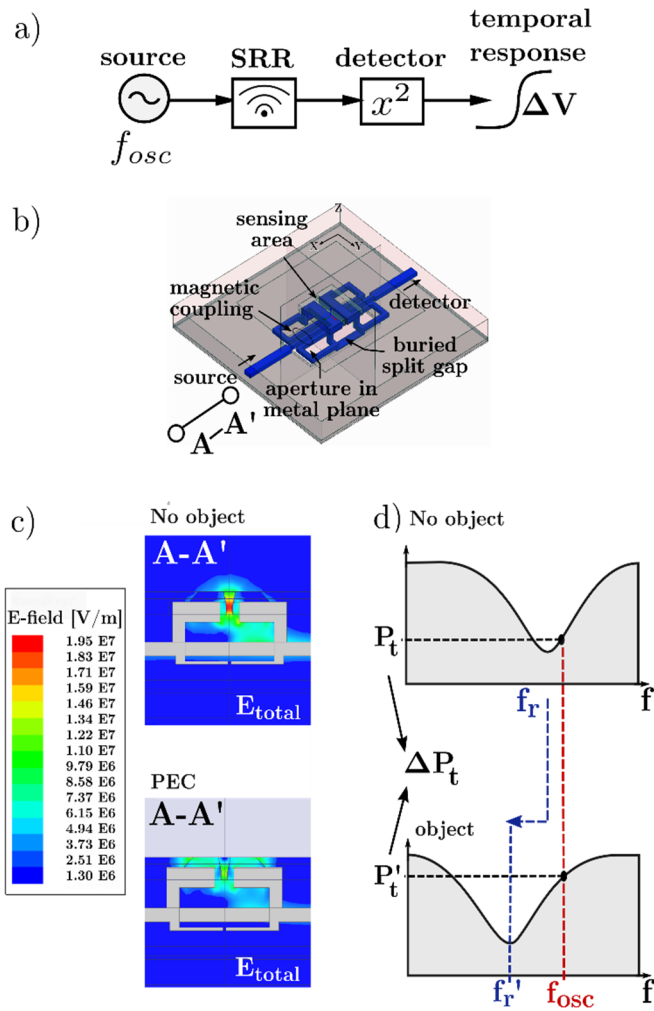


Fig. 3. a) 3-D illustration of the SRR topology. b) Pixel block-diagram and c) EM simulation of the resonator fields with no object and a perfect electrical conductor (PEC) placed on the top surface of the chip and illustration of the sensing principle.

with striplines to avoid any parasitic interactions with the sensed object. In order to maximize the array density, two rows of 64 pixels are vertically mirrored and offset by $25 \mu\text{m}$. With a $50 \mu\text{m}$ pixel pitch in one row, this gives a $25 \mu\text{m}$ pixel pitch for one direction in 2-D image acquisition. This results in a 1-D fill factor of 48% and around 100 dpi.

The THz wave is chopped at 200 kHz, and the detector signal is post-processed with a read-out chain based on lock-in techniques to avoid sensitivity deterioration caused by addition of detector and amplifier flicker noise. The globally shared read-out circuitry comprises a variable-gain bandpass amplifier, a CMOS switch mixer, a 3rd-order switched-capacitor low-pass filter and an instrumentation amplifier. The array can be operated in an analog read-out mode by monitoring the band-pass output signal or in a digital read-out mode that makes use of the entire on-chip analog lock-in circuitry and subsequent digitization with a 6-bit flash ADC. The array facilitates low-power operation by sequentially enabling a single TPO and detector and by sharing of the read-out circuitry between all pixels, resulting in a total power consumption of only 78 mW [5].

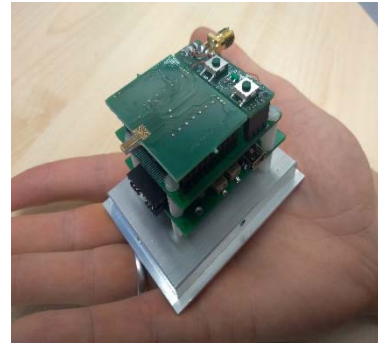


Fig. 4. Picture of the packaged portable near-field imager module. The portable module can be operated with a single USB interface.

The sensor is packaged with a standard wire-bonding process. In order to prevent physical damage or short circuits in wet material environments, the pads and wirebonds are encapsulated with preselected epoxy resin. As part of the technology process, a thin passivation layer with a thickness of around $2 \mu\text{m}$ provides a shielding layer between object and resonators. The imaging module consists of three stacked low-cost FR-4 boards, as shown in Fig 4. Additional electronics comprise a field-programmable-array (FPGA) for digital control of the chip and linear voltage regulators for the chip power supply. The chip continuously streams out the ADC values to the FPGA via SPI, which passes the output to a PC via USB after averaging and offset-correction. A digital video stream may be displayed by a dedicated video capture software.

III. RESULTS

The pixel performance was characterized using an on-wafer probe-station with different objects positioned above the sensing surface by means of a high precision 3-D translation stage. The dynamic range of the chip is 93 dB in a 1 Hz bandwidth at 200 kHz in analog read-out mode and 37 dB in digital read-out mode with 28 fps. The lateral resolution of the pixels is estimated to be between $10 \mu\text{m}$ and $12 \mu\text{m}$ [4].

The sensor response is a function of the material dependent electrical field disturbance in the sensing volume of the resonator. For imaging objects with homogeneous dielectric permittivity, the sensor can be used for μm -scale profilometry by mapping the decay of the electrical field strength and the resulting sensor response to the sensor-to-object distance. Whilst absolute distance measurements require thorough calibration as well as accurate reference measurements of the objects dielectric permittivity, relative measurements are sufficient for applications that aim to distinguish characteristic features. As one such example we demonstrate the array as a tool for biometrical fingerprint data acquisition.

Fig. 4 shows an optical image of an ink-and-paper fingerprint, as well as a THz near-field image of the same finger. For image acquisition, the near-field array was translated in a continuous 1-D movement along the direction orthogonal to the sensing stripe. The finger was in direct contact with the chip surface without the support of any high-precision mechanical setup. The on-chip digital read-out was utilized for data logging and was operated with a speed of 15 fps. A total image size of 842×128 pixels with a pixel pitch of

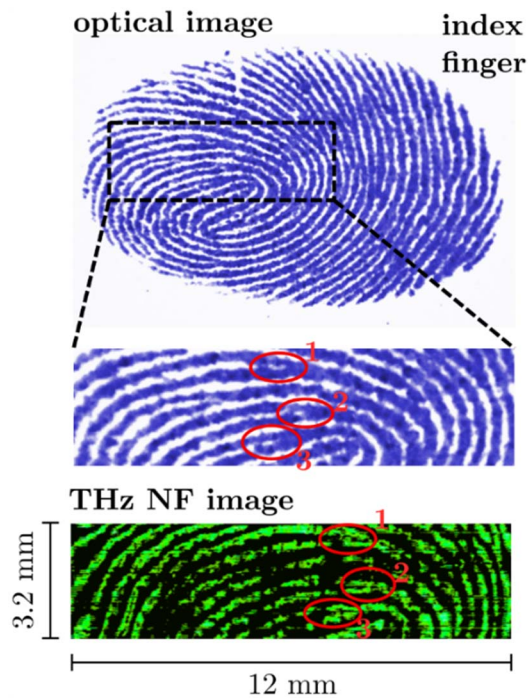


Fig. 5. Optical image of an ink-and-paper fingerprint and a THz near-field image. The ridges and characteristic ridge splits (marked as 1,2,3) are clearly resolved. The array was mounted to a 1-D translation stage. Data was acquired with continuous 1-D movement. Image size = 842 x 128, $T_{scan} \approx 30s$.

25 μm in Y-direction and 14.25 μm in X-direction was acquired in a scanning time of about 30s. The results clearly demonstrate that the characteristic ridges and groves, sized between 100-250 μm , can be easily resolved by the near-field scanner. Similarly, three characteristic ridge splits can be identified in the THz image. Note, that the image is substantially oversampled and that the image acquisition can be reduced to 5s without losing information. The measurements were repeated multiple times with no damage of the sensing surface. However, after each scan, particle leftovers were removed with isopropanol.

IV. CONCLUSION

To the authors best knowledge, this work shows the first demonstration of biometric fingerprint reading based on THz near-field sensing. Although only a 1-D array was implemented in this work, the image quality is comparable to commercially available capacitive fingerprint sensors [7]. An all-electronic near-field sensor module comprising multiple pixels was integrated in low-cost silicon technology for acquisition of the fingerprint profile. The module enables real-time scanning of the reactive near-field interaction between a sample and 128 on-chip split-ring-resonators. Aside from fingerprint recognition, silicon-based near-field sensors can potentially be used in applications like in-situ imaging of breast cancer margins [8] or conductivity characterization in semiconductor fabrication [9]. Moreover, the compact co-integration of a large-scale THz front-end with on-chip analog and digital signal post-processing indicates the potential of silicon technology for implementation of advanced THz systems that can be handled like conventional consumer electronics.

REFERENCES

- [1] A. J. L. Adam, "Review of Near-Field Terahertz Measurement Methods and Their Applications," *Journal of Infrared, Millimeter, and Terahertz Waves*, vol. 32, no. 8-9, pp. 976-1019, sep 2011.
- [2] Chen, Hou-Tong, Roland Kersting, and Gyu Cheon Cho. "Terahertz Imaging with Nanometer Resolution," *Applied Physics Letters*, vol. 83, no. 15, pp. 3009-3011, 2011.
- [3] J. Grzyb, B. Heinemann and U. R. Pfeiffer, "A 0.55 THz Near-Field Sensor With a μm -Range Lateral Resolution Fully Integrated in 130 nm SiGe BiCMOS," *Journal of Solid-State Circuits*, vol. 51, no. 12, pp. 3063-3077, Dec. 2016.
- [4] J. Grzyb, B. Heinemann and U. R. Pfeiffer, "Solid-State Terahertz Superresolution Imaging Device in 130-nm SiGe BiCMOS Technology," *Transactions on Microwave Theory and Techniques*, vol. 65, no. 11, pp. 4357-4372, Nov. 2017.
- [5] P. Hillger *et al.*, "A 128-pixel 0.56THz sensing array for real-time near-field imaging in 0.13 μm SiGe BiCMOS," *2018 IEEE International Solid-State Circuits Conference - (ISSCC)*, San Francisco, CA, 2018, pp. 418-420.
- [6] H. Rucker, B. Heinemann and A. Fox, "Half-Terahertz SiGe BiCMOS technology," *2012 IEEE 12th Topical Meeting on Silicon Monolithic Integrated Circuits in RF Systems*, Santa Clara, CA, 2012, pp. 133-136.
- [7] H. Y. Tang *et al.*, "3-D Ultrasonic Fingerprint Sensor-on-a-Chip," in *IEEE Journal of Solid-State Circuits*, vol. 51, no. 11, pp. 2522-2533, Nov. 2016.
- [8] Quentin Cassar, Amel Al-Ibadi, Laven Mavarani, Philipp Hillger, Janusz Grzyb, Gaetan MacGrogan, Thomas Zimmer, Ullrich R. Pfeiffer, Jean-Paul Guillet, and Patrick Mounaix, "Pilot study of freshly excised breast tissue response in the 300 - 600 GHz range," *Biomed. Opt. Express* 9, pp. 2930-2942, 2018
- [9] A. J. Huber, F. Keilmann, J. Wittborn, J. Azpurua and R. Hillenbrand, "Terahertz Near-Field Nanoscopy of Mobile Carriers in Single Semiconductor Nanodevices," *Nano Letters* 8 (11), pp. 3766-3700, 2008